

Evolution from first-order valence transition to heavy-fermion behavior in $\text{YbIn}_{1-x}\text{Ag}_x\text{Cu}_4$

J. L. Sarrao, C. D. Immer, C. L. Benton, and Z. Fisk

National High Magnetic Field Laboratory, Florida State University, 1800 E. Paul Dirac Drive, Tallahassee, Florida 32306

J. M. Lawrence

Department of Physics, University of California, Irvine, Irvine, California 92717

D. Mandrus* and J. D. Thompson

Materials Science and Technology Division, Los Alamos National Laboratory, Los Alamos, New Mexico 87545

(Received 7 May 1996)

YbInCu_4 undergoes a first-order isostructural valence transition near 40 K, whereas YbAgCu_4 is a moderately heavy ($\gamma=250$ mJ/mol K²) mixed-valence compound. We have succeeded in growing single crystals of these compounds, as well as many intermediate alloys, using flux-growth techniques. The evolution from YbInCu_4 to YbAgCu_4 has been characterized using electrical resistivity, magnetic susceptibility, and x-ray powder diffraction. The data are interpreted in terms of the evolution of the single-impurity Kondo temperature as a function of Ag concentration. [S0163-1829(96)07841-1]

I. INTRODUCTION

Since being discovered by Felner and Nowik,¹ YbInCu_4 has continued to attract attention.² YbInCu_4 is the only stoichiometric compound yet discovered that undergoes a first-order isostructural valence transition at ambient pressure. At high temperature ($T>50$ K) Yb is trivalent, displaying Curie-Weiss susceptibility with paramagnetic moment near the free-ion value of $4.5\mu_B$. At the first-order transition, the Yb valence is reduced to approximately 2.9 (as estimated by x-ray absorption and lattice constant measurements¹), with a consequent increase in lattice volume of 0.5% and a reduction in magnetic susceptibility and spin disorder scattering. Recent high-resolution neutron diffraction measurements have confirmed that YbInCu_4 retains its $C15b$ structure below the transition temperature.³ On the other hand, isostructural YbAgCu_4 (Refs. 4 and 5) is a moderately heavy ($\gamma=250$ mJ/mol K²) mixed-valence compound whose susceptibility, field-dependent magnetization, and specific heat are consistent with a $J=7/2$ Kondo impurity, as described by the Coqblin-Schrieffer model.^{6,7}

The prototypical example of the type of first-order isostructural valence transition observed in YbInCu_4 is the so-called γ - α transition in elemental Ce (for a review, see, e.g., Refs. 8 and 9). Two isostructural face-centered-cubic phases of Ce metal are separated in pressure-temperature space by a line of first-order transitions which terminates at a critical point. In the low-density γ phase ($a_0=5.15$ Å) the Ce ions are essentially trivalent, but in the high-density α phase ($a_0=4.85$ Å), Ce is nearly tetravalent. Thus, in addition to a large ($\approx 15\%$) volume change, a reduction in magnetic susceptibility occurs at the transition. The actual valence of α -Ce is estimated to be 3.3.¹⁰ Several mechanisms have been proposed for the transition. Promotional models¹¹ argue for an explicit change in electronic configuration from $4f^1$ to $4f^0$ (i.e., a complete loss of f character). In a Mott transition picture,¹² the $4f$ electron retains its f character, but changes from localized to bandlike at the γ - α transition. Although

both models qualitatively explain the physics of the transition, the energy scales for both are charge fluctuation energies, which appear to be too large to provide a complete and quantitative explanation. On the other hand, the Kondo volume-collapse (KVC) model¹³ has spin fluctuations as its characteristic excitation. This model exploits the Kondo aspects of the Anderson impurity Hamiltonian. Qualitatively, the first-order transition arises because of the strong volume dependence of the Kondo temperature.

Despite such study, many details, both experimental and theoretical, are unresolved. Experimentally, detailed measurements are difficult because most systems which display such a transition require either greater than ambient pressure (below 3 kbar the β phase of Ce interferes with the γ - α transition) or nonstoichiometry ($\text{CeNi}_{1-x}\text{Co}_x\text{Sn}$, $x\approx 0.3$, being the most recently discovered example¹⁴ of such a valence transition). Theoretically, although the physics of the KVC model derives from the Kondo impurity picture, a direct solution in terms of the Anderson impurity Hamiltonian is not available. Thus $\text{YbIn}_{1-x}\text{Ag}_x\text{Cu}_4$ is an attractive system because the valence transition occurs in the stoichiometric material YbInCu_4 at ambient pressure and the properties of YbAgCu_4 can be quantitatively explained in terms of a $J=7/2$ Kondo impurity model. As a practical matter, the samples are also less prone to oxidation and other extrinsic effects than previously studied Ce alloys.

There are, of course, complications. Controversy exists as to the precise value of the transition temperature T_v in YbInCu_4 —values ranging from 40 to 80 K have been reported—and to the evolution of the transition upon doping away from the stoichiometric compound.^{1,2,15} For YbAgCu_4 , although the physics is well described by the single-impurity model, there exist some quantitative self-consistency problems related to the particular measurement used to extract the Kondo temperature.⁵ In an attempt to shed some light on these issues as well as to understand the evolution from first-order valence change to mixed valence as Ag is substituted for In, we have synthesized single crystals of and performed

various physical measurements on $\text{YbIn}_{1-x}\text{Ag}_x\text{Cu}_4$. The data are interpreted in terms of the evolution of the Kondo temperature as a function of Ag concentration. A preliminary account of these data has already been given.¹⁶

II. YbInCu_4

Single crystals of YbInCu_4 were grown by combining stoichiometric ratios of the constituent elements in a 1:1 ratio with InCu flux. The high-purity materials (minimum 99.99% purity) were placed in an alumina crucible and sealed in an evacuated quartz tube. The sample was then heated to 1100 °C and cooled slowly (20 °C/h) to 800 °C, at which point the excess flux was spun off with a centrifuge, leaving tetrahedrally shaped crystals with a typical dimension of several millimeters. Although the above receipt has been the most fruitful in terms of size and quality of crystals, the composition and concentration of the flux do not appear to be critical parameters. Various Cu:In ratios between 1:1 and 2:1 have been used successfully as a flux, and compound to flux ratios from 1:1 to 1:3 have also been used. We have, however, been unable to produce crystals using only an excess In flux.

The first-order valence change in YbInCu_4 can be clearly seen in the evolution of the magnetic susceptibility and relative length change as a function of temperature in our flux-grown crystals.^{3,16} The magnetic susceptibility changes from Curie-Weiss behavior to being essentially independent of temperature and the volume of the sample increases by approximately 0.5% over a very narrow temperature range. The midpoint of the transition occurs at $T_v=42$ K with a 10%–90% width of less than 2 K. All of our crystals produced in the manner described above have transition temperatures between 40 and 45 K with maximal widths of 5 K. Our crystals show no evidence for transitions in the 50–80 K range as reported by others² and as observed by us for samples made on stoichiometry in sealed Ta tubes.³ Presumably, the difference in both sharpness and position of the valence transition is due to the lower temperature at which the crystals are produced and the consequent ordered nature of our crystals, as evidenced by their highly faceted morphology. Structural refinements based on neutron powder diffraction data³ suggest that polycrystalline samples with higher T_v and broader transitions possess approximately 10% disorder on the Yb and In sites, whereas our flux-grown single crystals have only 2%–3% disorder.

The electrical resistivity of YbInCu_4 (Fig. 1) is semimetallic at high temperature and shows a large and hysteretic drop at T_v . On thermal cycling through the transition, the high-temperature resistance of the sample increases substantially, presumably due to the buildup of internal strain associated with the volume contraction on going from the low-temperature phase to the high-temperature phase. Because this effect can be reversed with rather modest anneals (several hours at 300 °C), microcracking of the sample is not indicated.

III. $\text{YbIn}_{1-x}\text{Ag}_x\text{Cu}_4$

We have also synthesized single crystals of $\text{YbIn}_{1-x}\text{Ag}_x\text{Cu}_4$ for the full range of x values ($0 \leq x \leq 1$) in a

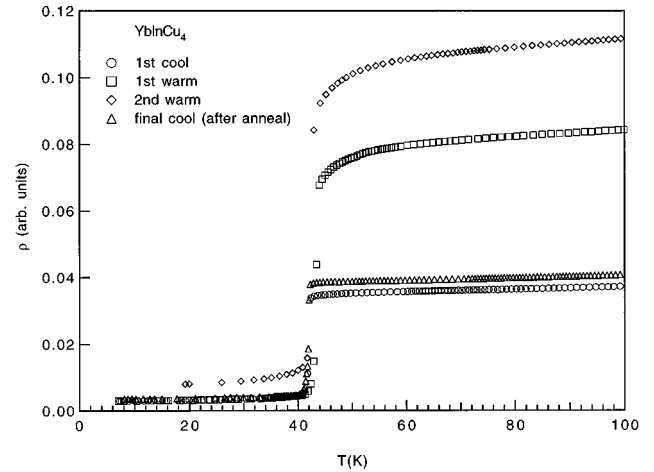


FIG. 1. Electrical resistivity of YbInCu_4 as a function of temperature. On thermal cycling the high-temperature resistivity increases, presumably because of strain effects. Annealing reverses these effects. See text for details.

similar manner. To produce $\text{YbIn}_{1-x}\text{Ag}_x\text{Cu}_4$ crystals, a combined flux and compound composition of $\text{YbIn}_{2-2x}\text{Ag}_{2x}\text{Cu}_5$ (analogous to the YbIn_2Cu_5 used to grow YbInCu_4) is used. Electron microprobe analysis confirms that the actual Ag:In ratio in the grown crystals is consistent with the nominal composition. Both YbInCu_4 and YbAgCu_4 , as well as all intermediate alloys, crystallize in the face-centered-cubic $C15b$ structure as evidenced by the observation of the (200) and (420) reflections in the x-ray powder diffraction patterns for our crystals. In the $C15$ structure, in which independent Yb and In/Ag sublattices do not exist, these reflections are forbidden.

The room-temperature lattice parameter as a function of Ag concentration for $\text{YbIn}_{1-x}\text{Ag}_x\text{Cu}_4$ is shown in the inset of Fig. 2. Vegard's law is not obeyed over the full range of concentrations. Rather, the lattice constant is essentially independent of x for Ag concentrations less than $x=0.5$. For

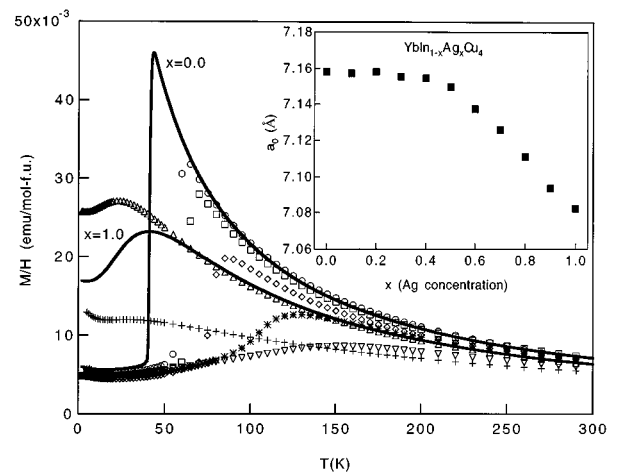


FIG. 2. Magnetic susceptibility [in units of emu/mol formula unit] as a function of temperature for $\text{YbIn}_{1-x}\text{Ag}_x\text{Cu}_4$ at various x ($x=0.1$ (○), $x=0.15$ (□), $x=0.2$ (◇), $x=0.3$ (*), $x=0.4$ (▽), $x=0.6$ (+), and $x=0.8$ (△)). Inset: cubic lattice constant at room temperature as a function of x for $\text{YbIn}_{1-x}\text{Ag}_x\text{Cu}_4$.

larger values of x , the lattice constant decreases linearly with increasing Ag concentration. Apparently, as the smaller Ag substitutes for the larger In, the size (and hence average valence) of Yb adjusts (Yb^{2+} is larger than Yb^{3+}) so as to keep the overall lattice parameter constant. For Ag concentrations greater than 0.5, the maximal valence compensation has occurred, the Yb valence remains constant, and a linear dependence of the lattice constant on dopant concentration is recovered. This will be discussed in greater detail in Sec. IV.

The nonlinear evolution of the physical properties of $\text{YbIn}_{1-x}\text{Ag}_x\text{Cu}_4$ with increasing Ag concentration is also apparent from measurements of the low-temperature linear coefficient of specific heat. Pillmayr *et al.* have measured γ as a function of x for a limited range of Ag concentrations.¹⁷ They observe that $\gamma=50$ mJ/mol K² and is approximately independent of x for $x<0.3$; γ for YbAgCu_4 is 250 mJ/mol K². Thus, at low temperature, the valence of Yb does not change, at least initially, with Ag substitution. This low-temperature behavior is in contrast with the initial change in valence of Yb at room temperature suggested by our lattice constant data.

The magnetic susceptibility χ as a function of temperature for representative Ag concentrations is shown in Fig. 2. Initially, T_v increases with Ag concentration, reaching an estimated critical concentration at $x=0.2$, with $T_v=60$ K. With further doping the sharp low-temperature drop in susceptibility is broadened and reduced in magnitude, until, near $x=0.5$, the susceptibility is nearly T independent. As the Ag concentration is further increased, a peak characteristic of a $J=7/2$ Kondo impurity begins to develop at low temperature. The temperature at which the peak occurs increases with increasing Ag concentration. For full Ag substitution, the peak occurs at $T=42$ K, slightly higher than but qualitatively consistent with previous reports.^{4,5} Note that, similar to the effects observed in the low-temperature specific heat,¹⁷ $\chi(0)$, the susceptibility as $T\rightarrow 0$, is essentially unchanged with x for $x<0.5$ before changing substantially with increasing x .

Effects similar to those in the magnetic susceptibility are observed in the temperature dependence of the electrical resistivity as a function of x [Fig. 3(a)]. Initially ($x=0$), a sharp and hysteretic drop in resistance at T_v is observed. (For clarity, only measurements made on initial cooling are shown.) At intermediate x , the resistance as a function of temperature is relatively flat, due presumably to Ag-In site disorder. Finally, for $x=1$ a coherence-induced drop in the resistance near 50 K is observed. The magnitude of the room-temperature electrical resistivity of YbAgCu_4 is approximately 4 times less than that of YbInCu_4 [Fig. 3(b)]. There also appears to be a peak in the room-temperature resistivity as a function of x near $x=0.1$. This, perhaps coincidentally, is near the concentration at which the valence transition becomes continuous. On the other hand, at low temperatures the resistivity is smaller for the stoichiometric ternary compounds, consistent with increased residual resistivity due to In/Ag disorder.

IV. DISCUSSION

The evolution of the physical properties of $\text{YbIn}_{1-x}\text{Ag}_x\text{Cu}_4$ as a function of temperature can be under-

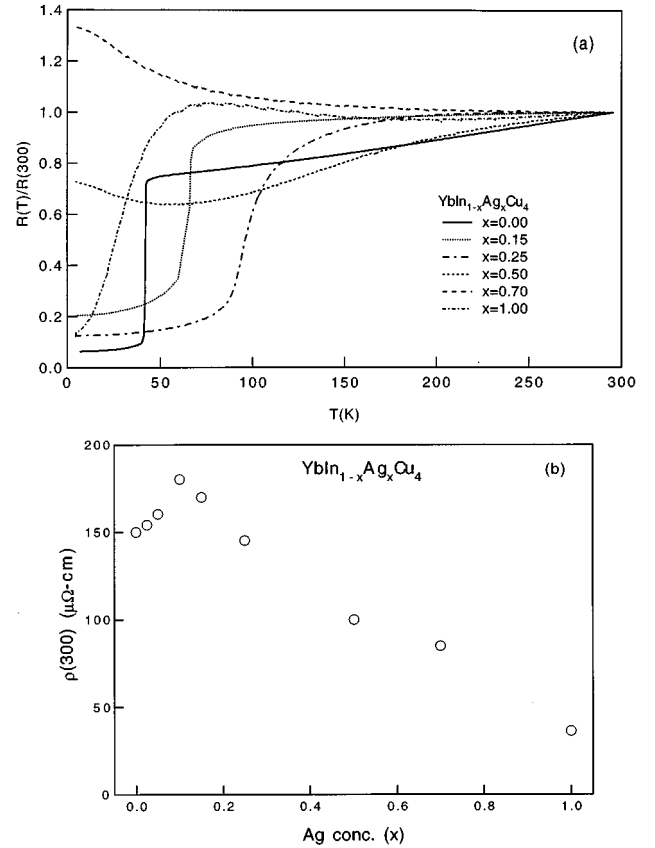


FIG. 3. Electrical resistivity as a function of temperature for $\text{YbIn}_{1-x}\text{Ag}_x\text{Cu}_4$ at various x . The upper panel (a) shows the normalized resistance as a function of temperature, and the lower panel (b) gives the room-temperature resistivity.

stood, at least qualitatively, in terms of the Kondo impurity model. In the limit of weak interactions between the $4f$ sites (the YbAgCu_4 limit), the system will be characterized by a single value of characteristic (Kondo) energy T_K . The effective moment $f \equiv \chi T/C$ (where C is the $J=7/2$ Curie constant for Yb), the specific heat, and the $4f$ hole occupation $n_f(T)$ (related to the Yb valence z , by $z=2+n_f$) will scale with T/T_K , as expected for the single impurity Anderson model,¹⁸ and n_f will evolve smoothly from a value of order 0.8–0.9 at $T=0$ towards unity at high temperature. Because the divalent Yb ion is larger than the trivalent ion, the cell volume v should vary proportionally to n_f . When a cell fluctuates to a larger value of n_f , a long-range strain field is set up such that an additional pressure is exerted on the lattice, which makes the increase of $n_f(T)$ and hence the decrease of v more rapid than in the noninteracting limit. This gives rise to an effective f - f interaction, which can be incorporated in a Landau functional;^{8,19} sufficiently strong effective interactions can cause a first-order transition (the YbInCu_4 limit). Any parameter such as alloy concentration which weakens the interactions will drive the first-order transition to a critical point, beyond which the transitions will be continuous.^{8,19}

For $\text{YbIn}_{1-x}\text{Ag}_x\text{Cu}_4$ we plot the effective moment $f \equiv \chi T/C$ in Fig. 4, where it can be seen that the transition is first order (discontinuous) for $x=0.1$, but continuous for $x=0.3$. To estimate the critical concentration x_c , we note that the maximum derivative $(df/dT)_{\text{max}}$ for samples with

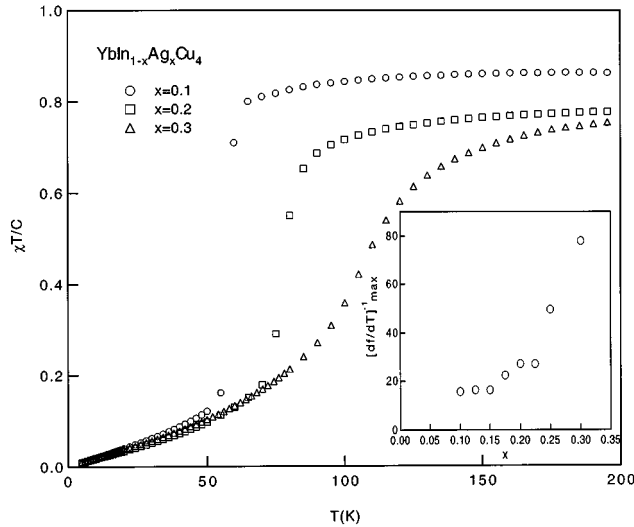


FIG. 4. The effective moment $f \equiv \chi T / C$ vs temperature for $\text{YbIn}_{1-x}\text{Ag}_x\text{Cu}_4$ for $x=0.1$, 0.2 , and 0.3 . The phase transition is discontinuous for $x=0.1$ and continuous for $x=0.3$. Inset: the inverse of the maximum derivative of the effective moment, $1/(df/dT)_{\max}$ for several x for which the transitions are continuous; this extrapolates to zero at the critical concentration x_c .

continuous transitions should diverge as $x \rightarrow x_c$ ($T \rightarrow T_v$). Plotting $1/(df/dT)_{\max}$ vs x in the inset of Fig. 4, we see that the critical concentration is $x_c \approx 0.2$. This estimate corresponds experimentally to the Ag concentration above which no hysteresis (of the type shown in Fig. 1) is observed in electrical resistivity measurements.

Alloying with Ag thus weakens the interactions responsible for the first-order transition, without diluting the Yb sublattice. Because the parameter x_c is a measure of how rapidly the interactions are reduced, a study of the variation of x_c with solute (Ag, Zn, Sn, etc.) might clarify which aspects of the underlying electronic structure affect the interactions responsible for the first order transition. The peak in room-temperature resistivity near the critical concentration suggests that low carrier density may play a significant role in this regard.

In the Kondo volume collapse (KVC) model of the Ce γ - α transition, Allen and Martin¹³ argue that the valence transition is driven by variation of the characteristic energy T_K as the cell volume varies: T_K depends on the hybridization V_{fc} between the Yb $4f$ and the conduction electrons, while V_{fc} depends on cell volume v . In YbInCu_4 the change in characteristic energy at $T_v = 42$ K is discontinuous, from a small value characteristic of nearly trivalent (heavy fermion) Yb for $T > T_v$ to a larger value characteristic of weak ($n_f \approx 0.85$) mixed valence for $T < T_v$. To estimate the characteristic energy we fit the effective moment to the prediction⁷ of the $J=7/2$ Kondo model [Fig. 5(a)]. The quantity T_L represents one way of defining the Kondo temperature; it is related theoretically to the low-temperature susceptibility by $T_L \equiv C/\chi(0)$ and to the temperature T_0 used by Rajan⁷ by $T_L = [2\pi/(2J+1)]T_0$. The values obtained, 20 K for the high-temperature state and 430 K for the low-temperature state, are in reasonable agreement with the values (26 and 480–540 K) obtained from inelastic neutron scattering measurements.^{20,21}

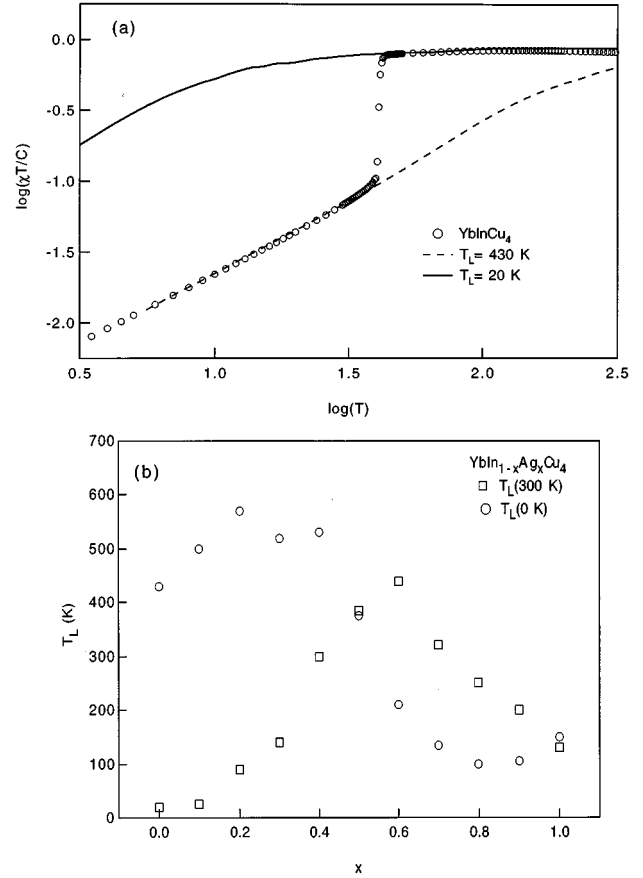


FIG. 5. (a) The effective moment vs temperature (plotted on logarithmic scales) for YbInCu_4 is compared to the prediction of the $J=7/2$ Kondo model for a Kondo temperature $T_L=20$ K in the high-temperature state and for $T_L=430$ K in the low-temperature state. (b) The low-temperature [$T_L(0\text{ K})$] and room-temperature [$T_L(300\text{ K})$] Kondo temperatures for $\text{YbIn}_{1-x}\text{Ag}_x\text{Cu}_4$ derived as in part (a).

For continuous transitions, the variation of T_K with temperature should be continuous, as observed in neutron scattering studies²² of the γ - α transition in $\text{Ce}_{0.7}\text{Th}_{0.3}$. To find T_L at any temperature and any x for $\text{YbIn}_{1-x}\text{Ag}_x\text{Cu}_4$, we note that in the Kondo regime, the effective moment is a universal, monotonic function of T/T_L ; hence, for a given temperature there is a one-one relation between $\chi T / C$ and T_L . For $T_L(x; T)$ derived in this manner, the discontinuous change in T_L observed for small x [Fig. 5(a)] becomes continuous for $x > x_c \approx 0.2$; i.e., $T_L(T)$ becomes a smooth function of temperature. In Fig. 5(b) we show the values of T_L derived in this fashion at the lowest temperatures [$T_L(0\text{ K})$] and at room temperature [$T_L(300\text{ K})$] for the full range of x values. Because the evolution of the susceptibility with temperature is rather smooth, there is some uncertainty in the precise value of the fitted T_L ; however, varying T_L by 10 K produces a visibly worse fit.

For small x the room-temperature value $T_L(300\text{ K})$ increases rapidly with x , approaching the low-temperature value $T_L(0\text{ K})$ (which changes less dramatically with x , consistent with the specific heat results of Pillmayr *et al.*¹⁷) at $x=0.5$. The increase in $T_L(300\text{ K})$ undoubtedly corresponds to an increase in the degree of mixed valence at room temperature. This would seem to confirm our hypothesis con-

cerning the lattice constant of $\text{YbIn}_{1-x}\text{Ag}_x\text{Cu}_4$: The increased mixed valence and corresponding size increase of the Yb ion precisely cancels the decrease in lattice size expected on the basis of Vegard's law. It would be worthwhile to confirm this argument by direct measurement of the valence $n_f(x, T)$, e.g. by L_{III} x-ray absorption. This tendency for $T_L(300 \text{ K})$ to approach $T_L(0 \text{ K})$ as x increases is consistent with the picture given above that when the interactions become sufficiently weak the Yb 4f electrons should decouple (to the extent that single-ion Kondo behavior should dominate). Initially, this appears to occur at $x=0.5$, where the data can be described by the Kondo theory with a single value of $T_L \approx 375 \text{ K}$ at all temperatures. It occurs again at $x=1$, i.e., for YbAgCu_4 , for which single-ion Kondo behavior is already known⁴ to be approximately valid.

For $0.5 < x < 1$ the characteristic temperature T_L appears to be larger at room temperature than at low temperature. This is unusual: The difference between $T_L(300 \text{ K})$ and $T_L(0 \text{ K})$ is larger than typically observed and is the opposite of what is observed for smaller Ag concentrations. An increase in T_L usually corresponds to an increase in the degree of mixed valence, and L_{III} x-ray absorption measurements²³ in several Yb compounds have confirmed that, as predicted for the Anderson model, the Yb becomes *less* mixed valent as the temperature increases. We do not know what the origin of this effect is. It is possible that there is a local environment effect; i.e., some fraction of Yb atoms have local environments which promote a smaller characteristic energy T_L than in the rest of the matrix, and hence cause an additional increase of susceptibility at low temperature. Although visibly

small, extrinsic contributions to the low-temperature susceptibility due to magnetic impurities may also cloud the issue. Direct measurement by inelastic neutron scattering would help to confirm whether the characteristic energy is constant or actually increases with temperature for $x \geq 0.5$.

V. SUMMARY

We have studied the evolution of "mixed valence" from the isostructural valence transition of YbInCu_4 to the heavy fermion behavior of YbAgCu_4 . This evolution can be interpreted in terms of the single-impurity Anderson Hamiltonian with strong interactions (i.e., the Kondo volume collapse model). Although much work remains to be done to map the complete composition–pressure–magnetic-field-temperature phase diagram of this system, $\text{YbIn}_{1-x}\text{Ag}_x\text{Cu}_4$ provides a model system for the study of isostructural valence transitions and tests of the single-impurity Kondo model.

ACKNOWLEDGMENTS

The NHMFL is supported by the NSF and the state of Florida through cooperative agreement No. DMR-9016241. Work at Los Alamos was performed under the auspices of the U.S. Department of Energy. Some of us (J.L.S., C.D.I., C.L.B., Z.F., and J.M.L.) also gratefully acknowledge support from the NSF through Grant Nos. DMR-9501528 and DMR-9501529.

*Present address: Solid State Division, Oak Ridge National Laboratory, Oak Ridge, Tennessee 37831.

¹I. Felner and I. Nowik, Phys. Rev. B **33**, 617 (1986); I. Felner *et al.*, *ibid.* **35**, 6956 (1987); I. Nowik *et al.*, *ibid.* **37**, 5633 (1988).

²B. Kindler, D. Finsterbusch, R. Graf, F. Ritter, W. Assmus, and B. Luthi, Phys. Rev. B **50**, 704 (1994), and references therein.

³J. M. Lawrence, G. Kwei, J. L. Sarrao, Z. Fisk, D. Mandrus, and J. D. Thompson, Phys. Rev. B **54**, 6011 (1996).

⁴C. Rossel, K. N. Yang, M. B. Maple, Z. Fisk, E. Zirngiebl, and J. D. Thompson, Phys. Rev. B **35**, 1914 (1987).

⁵T. Graf, J. M. Lawrence, M. F. Hundley, J. D. Thompson, A. Lacerda, E. Haanappel, M. S. Torikachvili, Z. Fisk, and P. C. Canfield, Phys. Rev. B **51**, 15 053 (1995).

⁶P. Schlottmann, J. Appl. Phys. **73**, 5412 (1993).

⁷V. T. Rajan, Phys. Rev. Lett. **51**, 308 (1983).

⁸J. M. Lawrence, P. S. Riseborough, and R. D. Parks, Rep. Prog. Phys. **44**, 1 (1981).

⁹D. C. Koskenmaki and K. A. Gschneider, in *Handbook on the Physics and Chemistry of the Rare Earths*, edited by K. A. Gschneider and L. Eyring (North-Holland, Amsterdam, 1978), Vol. 1, Chap. 4.

¹⁰J. Rohler, in *Handbook on the Physics and Chemistry of the Rare Earths*, edited by K. A. Gschneider and L. Eyring (North-Holland, Amsterdam, 1987), Vol. 10, p. 453.

¹¹L. M. Falicov and J. C. Kimball, Phys. Rev. Lett. **22**, 997 (1969).

¹²B. Johansson, Philos. Mag. **30**, 469 (1974).

¹³J. W. Allen and R. M. Martin, Phys. Rev. Lett. **49**, 1106 (1982); see also J. W. Allen and L. Z. Liu, Phys. Rev. B **46**, 5047 (1992).

¹⁴D. T. Adroja, B. D. Rainford, J. N. de Teresa, A. del Moral, M. R. Ibarra, and K. S. Knight, Phys. Rev. B **52**, 12 790 (1995).

¹⁵K. Kojima, H. Hayashi, A. Minami, Y. Kasamatsu, and T. Hihara, J. Magn. Magn. Mater. **81**, 267 (1989).

¹⁶J. L. Sarrao, C. L. Benton, Z. Fisk, J. M. Lawrence, D. Mandrus, and J. D. Thompson, Physica B **223&224**, 366 (1996).

¹⁷N. Pillmayr, E. Bauer, and K. Yoshimura, J. Magn. Magn. Mater. **104-107**, 639 (1992).

¹⁸N. E. Bickers, D. L. Cox, and J. W. Wilkins, Phys. Rev. B **36**, 2036 (1987).

¹⁹J. M. Lawrence, M. C. Croft, and R. D. Parks, in *Valence Instabilities and Related Narrow Band Phenomena*, edited by R. D. Parks (Plenum, New York, 1977), p. 35.

²⁰A. Severing, A. P. Murani, J. D. Thompson, Z. Fisk, and C.-K. Loong, Physica B **163**, 409 (1990).

²¹J. M. Lawrence, S. M. Shapiro, J. L. Sarrao, Z. Fisk, and J. D. Thompson (unpublished).

²²S. M. Shapiro, J. D. Axe, R. J. Birgeneau, J. M. Lawrence, and R. D. Parks, Phys. Rev. B **16**, 2225 (1977).

²³J. M. Lawrence, G. H. Kwei, P. C. Canfield, J. G. DeWitt, and A. C. Lawson, Phys. Rev. B **49**, 1627 (1994).